https://doi.org/10.2352/EI.2026.38.8.IQSP-254

From Centroid to Low-Pass Edge Fitting in ISO 12233 e-SFR: Accuracy and Impact on Digital Imaging Information Metrics

Sarah Kerr; Imatest LLC; Boulder, Colorado USA

Abstract

Edge localization plays a critical role in ISO 12233 e-SFR analysis, influencing both sharpness results and downstream information capacity metrics. This paper evaluates the accuracy of the standard centroid, low-pass filter, and matched filter-based localization methods across an ensemble of simulated slanted edge ROIs. Localization errors are quantified by benchmarking each method against ground truth, and their propagation to e-SFR results and information capacity is measured. Findings show that centroid fitting introduces angular bias under noise, leading to a degraded effective response, while low-pass filtering and matched filtering both maintain robust accuracy. These results highlight an under-characterized source of error in standards-based image quality analysis and provide a foundation for improved methods. The results support a closer alignment between edge analysis, information-theoretic models, and emerging metrics such as those proposed in ISO/WD 23654 (Digital Imaging — Information Metrics).

Introduction

The International Organization for Standardization (ISO) standard for system resolution and spatial frequency response of electronic still picture imaging, known as ISO 12233, defines terminology, test chart specifications, and methods for measuring spatial frequency response (SFR) [1]. In particular, the edge-based SFR (e-SFR) algorithm for measuring resolution has been widely adopted due to its measurement efficiency and robustness [2–4].

Furthermore, the e-SFR can also be used to calculate additional system performance metrics such as signal-to-noise ratio (SNR) and information capacity [5, 6]. These additional metrics enable a more comprehensive evaluation of modern imaging systems, which are increasingly deployed in machine vision applications such as autonomous driving, medical diagnostics, surveillance, and robotics. Notably, recent work demonstrates that information capacity can predict object detection accuracy more reliably than traditional metrics such as SFR50 [7].

A critical but underexamined step in the e-SFR framework is edge localization, where the position of the edge is estimated for each row of the region of interest (ROI). Errors in this step propagate through the pipeline, affecting the SFR, noise estimation, and derived metrics such as information capacity. Because information capacity has been shown to correlate with machine vision performance, errors in edge localization may lead to incorrect predictions of overall system performance.

This work investigates the effects of edge localization accuracy by comparing the standard ISO 12233 centroid, low-pass filter (LPF), and matched filter-based localization methods. The impact of edge localization error on SFR and information capacity measurements is evaluated to quantify error propagation and assess its implications for machine vision performance.

Background

Edge Localization as an Estimation Problem

The ISO 12233 e-SFR algorithm, defined in Annex D of reference [1], describes the process of measuring the system SFR from an ROI containing a slanted edge. This method relies on projecting pixel rows onto a common axis to form an oversampled edge spread function (ESF). The ESF is differentiated to obtain the line spread function (LSF) and transformed to yield the SFR [1]. This approach assumes accurate knowledge of the edge position in each row.

Edge localization, a critical precursor to the projection step in the e-SFR algorithm, can be viewed as a parameter estimation problem where the goal is to estimate the position of a step edge in noisy data. The observed signal is the convolution of the ideal edge with the system point spread function (PSF) corrupted by noise. Under this formulation, localization error arises from noise in the ESF and finite sampling, which violates the assumption of accurate knowledge of the edge position. Prior work has shown that errors in edge slope estimation introduce systematic bias in SFR measurements, effectively acting as a blur filter that reduces high-frequency response [8, 9].

Edge Localization Methods

Edge localization in the ISO 12233 e-SFR algorithm is performed using a centroid-based method. In this approach, the edge position for each row is estimated from the center of mass of the derivative of the signal profile for each row as shown in formula (1).

$$C_c(r) = \frac{\sum_{p=1}^{P-1} p[\phi(p+1,r) - \phi(p,r)]}{[\phi(p+1,r) - \phi(p,r)]} - 1/2 \quad (1)$$

where C is the estimated edge position from centroid method, r is the row or y pixel coordinate of the slanted edge ROI, p is the column or x pixel coordinate of the slanted edge ROI, P is the total number of pixels per row in the slanted edge ROI, and ϕ is the slanted edge ROI image [1]. This method is computationally efficient and widely used, but it is sensitive to noise as it depends on the distribution of gradient values. Per row localization errors from the centroid method are shown in Fig. 1(a-b).

An alternative approach is to apply an LPF to the signal profile of each row prior to differentiation and localization. By reducing high-frequency noise before differentiation, this method produces a smoother derivative signal and more stable estimate of the edge position. Although the LPF approach is less sensitive to noise than the centroid method and therefore introduces less bias to the estimated edge location, the filter is not tailored to the underlying signal structure and may still introduce some bias under noisy conditions.

A more general approach is to perform edge localization using matched filtering. In this framework, localization is based on correlation with an expected edge profile, rather than on generic

smoothing or centroid estimation. By incorporating a signal model, matched filtering improves resilience to noise and provides a model-based estimate with strong robustness to noise. This is consistent with optimal detection theory, where matched filtering maximizes signal response in the presence of additive noise[10].

Information Metrics and Machine Vision Performance

Information theory provides a principled framework for quantifying image quality in terms of task-relevant information transfer [11, 12]. In this framework, information capacity is derived from the signal power represented by SFR and noise power spectrum (NPS). Unlike SFR alone, information capacity accounts for noise statistics and frequency-dependent SNR in addition to signal contrast [5, 6]. The demonstrated correlation between information capacity and machine vision performance, particularly in object detection tasks [7], establishes a direct link between physical image quality factors and algorithmic performance. Since information capacity can be calculated from the same edge data used in e-SFR analysis [5, 6], errors in edge localization directly propagate into these higher-level information metrics, introducing bias in both signal and noise estimation. This establishes a direct causal pathway in which localization error propagates through SFR and noise estimation to information capacity, ultimately affecting predictions of machine vision performance.

Methods

Simulation of Slanted-Edge ROIs

A synthetic slanted edge dataset (N=1000) was simulated to evaluate edge localization accuracy under controlled imaging conditions. Each ROI was constructed from a high-resolution step edge then degraded using optical blur, sampling, and noise processes designed to approximate realistic camera behavior.

For each sample, an ideal slanted edge was generated on a 4x oversampled grid and then down sampled to the final ROI resolution after application of blur and noise. The final ROI dimensions were 128 x 256 pixels. Edge orientation, edge position, signal level, blur, and noise parameters were randomized independently for each ROI in order to produce a broad distribution of conditions.

The edge angle was sampled uniformly over a near-vertical range of 82° to 88°, defined relative to the horizontal image axis. The edge position was randomized by sampling a ± 8 pixel offset orthogonal to the edge orientation. The dark side signal level was sampled uniformly in the range [0.02, 0.23] and the bright side level was defined by a fixed contrast ratio of 4:1. This produced ROI contrast conditions consistent with e-SFR best practices while avoiding saturation.

Noise was added in multiple stages to approximate practical image acquisition. First, additive Gaussian noise was applied to the oversampled grid before applying optical blur to model signal perturbations such as illumination non-uniformity. Next, a sensor noise model was applied after optical blur and down sampling. An ISO value was determined through logarithmic uniform sampling over the range 100 to 124000 and exposure was then modeled as inversely proportional to ISO to maintain constant mean brightness. For each ROI, the effective electron count therefore decreased approximately as 100/ISO, and shot noise was applied through Poisson sampling of the corresponding electron counts. This represented shot-noise-limited image capture. Finally read noise was simulated by using zero-mean additive Gaussian noise. The RMS value sampled from 1.5 to 8 electrons.

Additionally, spatially correlated noise was then simulated by adding a demosaicing pipeline. Per channel gains were randomized for the Bayer raw image then the signal was mosaiced using an RGGB pattern. Gradient-corrected linear interpolation demosaicing was performed prior to luminance conversion using Rec. 709 weights. This process introduced realistic pixel-level correlation and demosaicing texture.

The final ROIs used to evaluate edge localization error were 16-bit single channel luminance. Ground truth edge parameters were retained for each ROI, enabling direct evaluation of edge

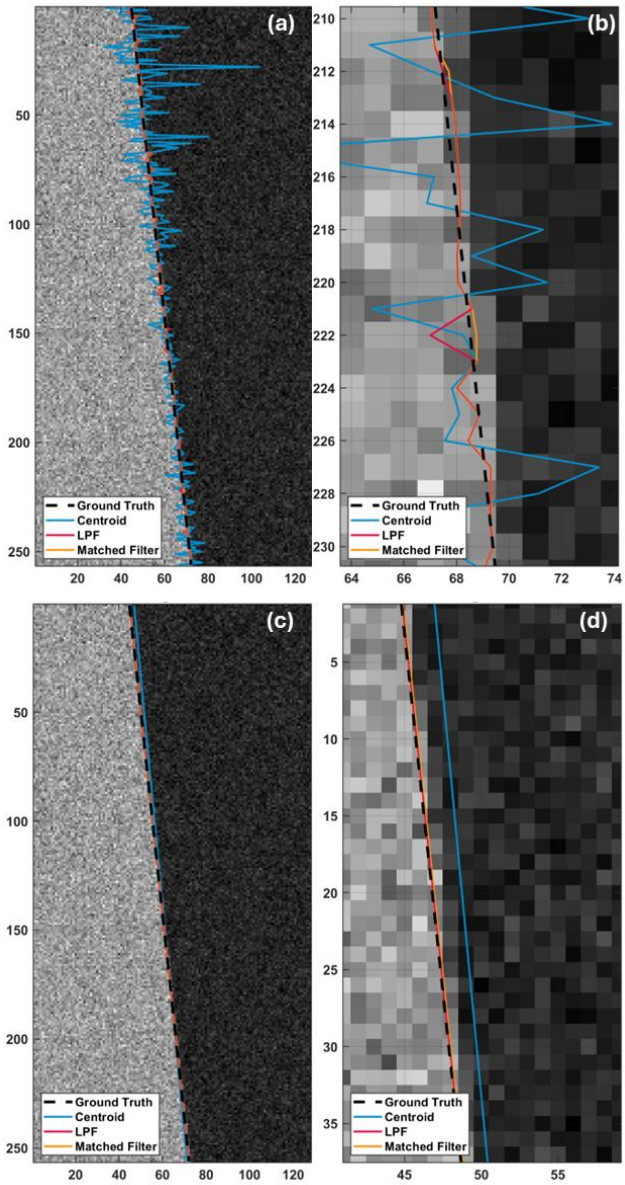

Figure 1 *Example edge-localization results for a sample simulated slanted-edge ROI (a) Full ROI showing row-wise edge estimates overlaid on a noisy edge; (b) magnified view of the same ROI illustrating the large row-to-row variability of the centroid estimate relative to ground truth, LPF, and matched-filter localization; (c) Full ROI showing linear fits to points shown in (a), and (d) corresponding magnified view. The centroid method exhibits larger angular bias and row-wise scatter, whereas LPF and matched filtering track the ground-truth edge more closely.*

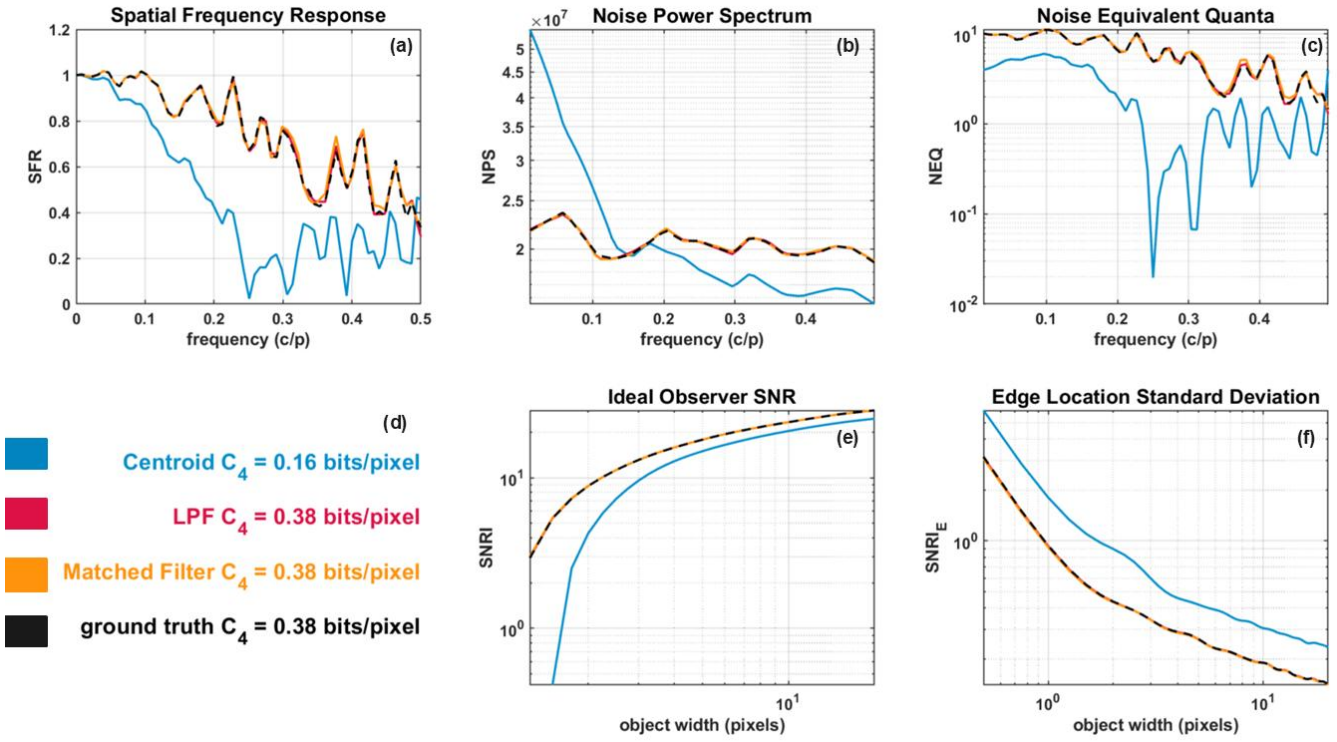

Figure 2 *Representative propagation of edge-localization error into downstream imaging metrics for the same simulated ROI as Fig. 1. Top row: spatial frequency response (SFR)(a), noise power spectrum (NPS) (b), and noise equivalent quanta (NEQ) (c) computed using centroid, LPF, matched-filter, and ground-truth localization. Bottom row: information capacity results (d), ideal observer signal-to-noise ratio integral (SNRI) as a function of object width (e), and edge-location standard deviation versus object width (f). Centroid localization reduces high-frequency SFR, distorts NPS, and underestimates information capacity (C_4), while LPF and matched filtering closely match ground truth.*

localization error. This simulation framework enabled direct measurement of localization error and its propagation into e-SFR and information-based metrics.

Edge Localization

Edge localization was performed using three methods: a centroid-based approach consistent with ISO 12233, an LPF approach, and a matched filter-based approach.

For the centroid method, the edge position for each row was estimated as shown in formula (1).

For the LPF method, a low-pass disk filter was applied to each row of the slanted edge ROI prior to differentiation to suppress high-frequency noise. The edge position was then estimated from the peak of the derivative of the smoothed ESF. The low-pass filter is applied as a convolution performed along the p-dimension for each row, r. That is,

$$C_l(r) = max_p \left[\frac{\mathrm{d}}{\mathrm{d}p}\left((\phi(\cdot, r) * h)(p)\right)\right] \tag{2}$$

where C_l is the estimated edge position from LPF method, r is the row or y pixel coordinate of the slanted edge ROI, p is the column or x pixel coordinate of the slanted edge ROI, ϕ is the slanted edge ROI image, and h is a circular averaging disk kernel. The radius of the disk kernel was selected empirically to balance noise suppression and edge broadening.

For the matched filter method, edge localization was performed using a two-stage process. First, a coarse estimate of the edge position for each row was obtained using the LPF method as described by formula (2). Each smoothed row was then aligned according to this coarse estimation of the edge location. Averaging over the aligned rows provided a low noise template ESF, as shown in formula (3).

$$t(p) = \frac{1}{R}\sum_{r=1}^{R}(\phi(\cdot, r) * h)(p - C_l(r)) \tag{3}$$

where t is the low noise template ESF, p is the column or x pixel coordinate of the slanted edge ROI, r is the row or y pixel coordinate of the slanted edge ROI, R is the total number of rows in the slanted edge ROI, ϕ is the slanted edge ROI image, h is a circular averaging disk kernel, C_l is the estimated edge position per row from LPF method.

The template ESF was differentiated and used to form a matched filter. The edge location in each row was estimated by maximizing the correlation applied along the p-dimension between the derivative of each row's signal profile and the template.

$$C_m(r) = max_p \left[\left(\frac{\mathrm{d}}{\mathrm{d}p}\phi(\cdot, r) \star \frac{\mathrm{d}}{\mathrm{d}p}t\right)(p)\right] \tag{4}$$

where C_m is the estimated edge position from matched filter method, r is the row or y pixel coordinate of the slanted edge ROI, p is the column or x pixel coordinate of the slanted edge ROI, ϕ is the slanted edge ROI image, and t is the low noise template ESF.

All three methods were applied to the same simulated ROIs then a linear fit was performed to obtain the final edge localization for each model. Fig. 1(c-d) provides a comparison of the edge fits from each localization method for a sample slanted edge ROI.

Localization accuracy was evaluated by comparison to the known ground-truth parameters and localization error was evaluated in terms of $\Delta\theta$, the angle between the localized edge and the ground truth edge, to quantify its direct impact on edge binning and SFR estimation.

SFR and Information Metric Computation

SFR was then computed for each edge localization method by applying the remaining steps of the ISO 12233 e-SFR algorithm. A comparison of SFR results from each edge localization method for a sample slanted edge ROI is presented in Fig. 2(a). Information metrics were computed using the same slanted-edge data used for e-SFR analysis, consistent with the proposed ISO/WD 23654 framework from reference [5].

Noise at the edge, $N(x)$, was then computed as the variance across the edge using the same line-scan data as the e-SFR calculation. To compute the noise power spectrum (NPS), a noise-reduced edge image was reconstructed by back projecting the ESF edge model derived from the same line-scan data. This reconstructed image was subtracted from the original ROI to form a noise image. Fourier analysis of this noise image was used to compute NPS, providing a frequency-domain representation of image noise. The NPS was normalized according to Parseval's theorem, such that its integral is consistent with the measured $N(x)$. Information capacity, C_4, and related metrics were then computed using the measured SFR and NPS. A comparison of information metric results from each edge localization method for a sample slanted edge ROI is presented in Fig. 2(b-f).

SFR-area and NPS-area, the integrated area under each respective curve from 0 to 0.5 cycles/pixel, were evaluated for each localization method to quantify the error introduced by localization error.

Results

Localization Accuracy

Edge localization accuracy was first evaluated by comparing the estimated edge position for each method to the known ground-truth edge parameters. The centroid method exhibited a systematic bias that increased with noise level, particularly at higher ISO conditions. The bias manifested primarily as an error in the estimated edge slope, resulting in a consistent misalignment of the projected edge data. This behavior is reflected in Fig. 3(a), where the centroid method has an angular-error center of 0.07° with a spread of 0.18° (N=983), compared with centers of 0.01° and spreads of 0.02° for both the LPF (N=999) and matched filter (N=1000) methods. Here, center and spread refer to the median and IQR values of the distributions.

In contrast, both the LPF and matched filter methods demonstrated improved robustness to noise. Across all simulated conditions, both LPF and matched filtering produce substantially lower localization error than the centroid method, with similar aggregate performance at the precision reported here. The 99% confidence ellipses in Fig. 3(a) show that the benefit of LPF and matched filtering is not limited to reduced mean error, but also includes a much tighter distribution of localization outcomes across the simulated conditions.

Impact on SFR

Localization error propagated directly into the e-SFR computation through the projection and binning process. Errors in edge slope resulted in misregistration of pixel data in the 4x oversampled binning space, producing a broadened ESF and corresponding attenuation of high-frequency content in the SFR.

The centroid method showed a consistent reduction in high-frequency SFR compared to the ground truth, with the effect increasing at higher noise levels. This behavior is consistent with an effective blur introduced by misalignment during edge projection. In Fig. 3(b), this appears as a broader joint distribution between angular error and SFR-area error for the centroid method, with an SFR-area center near 0.00 pixels^{-1} but a spread of 0.02 pixels^{-1} (N=983).

The LPF and matched filter methods reduced this effect, producing SFR estimates that more closely matched the ground-truth response. In Fig. 3(b), both the LPF and matched filtering methods reduce the spread to 0.01 pixels^{-1} (N=999, 1000), indicating more stable SFR estimations once edge localization is improved.

Impact on NPS

Differences in localization accuracy also affected the estimated noise power spectrum. Because the noise image is formed by subtracting a reconstructed noise-reduced edge from the original ROI, errors in edge localization introduce structured residuals that are interpreted as noise.

For the centroid method, localization error resulted in elevated low-frequency components in the NPS, reflecting the residual edge structure in the noise image. This led to an overestimation of noise power at low spatial frequencies. This effect is most evident in Fig. 3(c) where the centroid method has an NPS-area error center of 8890 DN^2/pixel^2 and a spread of 63800 DN^2/pixel^2 (N=983).

The LPF method reduced these artifacts by improving edge alignment, producing a more uniform and physically consistent NPS. The matched filter further minimized structured residuals, resulting in an NPS that more accurately reflected the underlying stochastic noise. In Fig. 3(c) the LPF and matched filter methods reduce the NPS-area error centers to 1692 and 1596 DN^2/pixel^2, respectively. The corresponding spreads were 10351 and 9971 DN^2/pixel^2 (N=999, 1000). Among the downstream metrics considered here, NPS-area error showed the largest absolute numerical separation between methods, indicating that NPS estimation is especially sensitive to edge-localization accuracy.

Impact on Information Capacity

The combined effects on SFR and NPS propagated into the information capacity metric. The centroid method consistently underestimated information capacity due to reduced high-frequency SFR and inflated low-frequency NPS. In Fig. 3(d), the centroid method has an information capacity error center of 0.01 bits/pixel with a spread of 0.03 bits/pixel (N=983).

The LPF and matched filter methods both improved information capacity estimates by reducing both signal attenuation and noise bias. In Fig. 3(d), both LPF and matched filter methods reduced the information capacity error center to 0.00 bits/pixel with spreads of 0.00 bits/pixel at the reported precision (N=999, 1000).

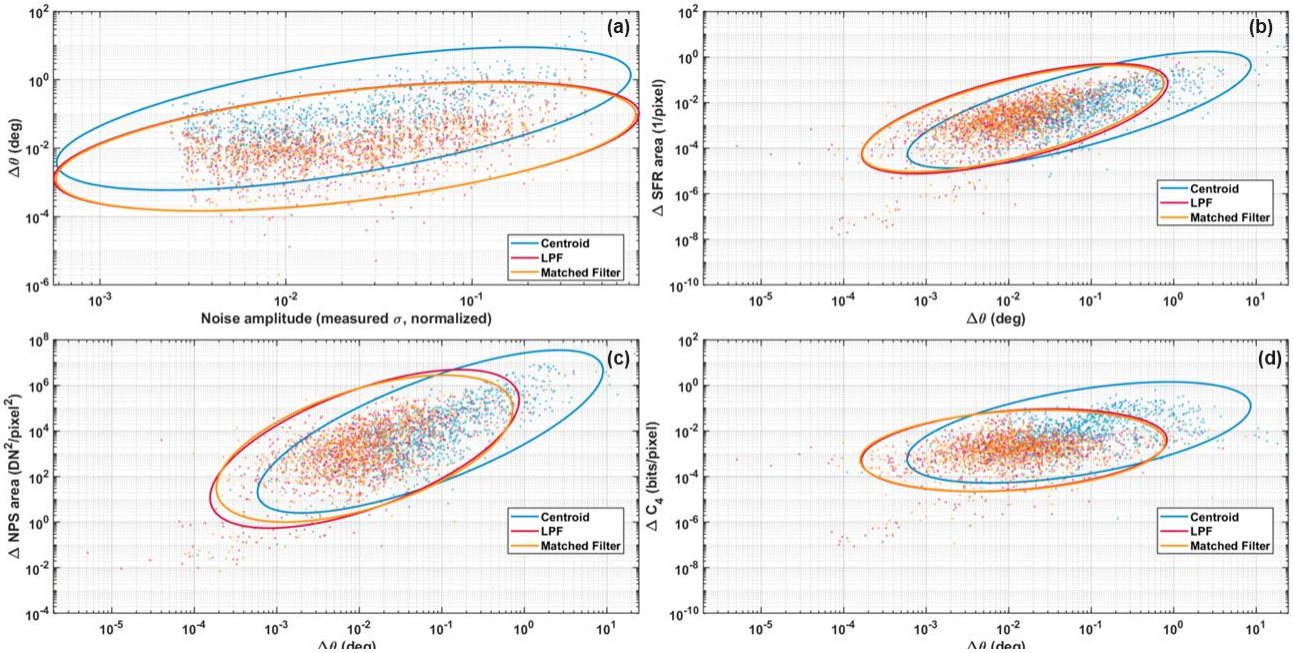

Figure 3 *Joint distributions of edge-localization error and downstream metric error across the simulated ROI ensemble. The panels plot noise amplitude versus angular localization error $\Delta\theta$ in (a), $\Delta\theta$ versus SFR-area error in (b), $\Delta\theta$ versus NPS-area error in (c), and $\Delta\theta$ versus information-capacity error ΔC_4 in (d) for centroid, low-pass-filtered (LPF), and matched-filter localization. The overlaid ellipses are 99% confidence ellipses for each method. Relative to centroid localization, LPF and matched filtering shift the distributions toward lower angular and downstream error and substantially reduce dispersion. For example, the centroid method has an angular-error center of 0.07 with spread 0.18, whereas both LPF and matched filtering have angular-error centers of 0.01 with spreads of 0.02. Likewise, the information-capacity error center decreases from 0.01 for centroid to approximately 0.00 for LPF and matched filtering, and the NPS-area error center decreases from 8890 for centroid to 1692 for LPF and 1593 for matched filtering. Sample counts were $N = 983$ for centroid, $N = 999$ for LPF, and $N = 1000$ for matched filtering.*

Taken together, the 99% confidence ellipses in Fig. 3(d) show that improved localization reduces not only the average bias in information capacity estimates, but also the uncertainty in those estimates across varying noise conditions.

Discussion

The results demonstrate that edge localization accuracy is a primary source of systematic error in e-SFR based image quality metrics. While the ISO 12233 framework assumes accurate knowledge of edge position, this work shows that practical localization methods introduce noise-dependent bias that propagates through the entire measurement pipeline. Edge localization error introduces bias in estimated edge slope, which leads to misregistration during projection and binning. This misregistration broadens the effective ESF, reducing high-frequency SFR. The same misalignment introduces structured residuals in the reconstructed noise image, inflating low-frequency NPS. These coupled effects propagate directly into information capacity, which depends jointly on SFR and NPS.

The centroid method, although widely used due to its simplicity and computational efficiency, was found to be particularly sensitive to noise. The observed angular bias results in misregistration during projection and binning, which manifests as an effective broadening of the edge profile. This leads to attenuation of high-frequency SFR and the introduction of structured residuals in the noise image, ultimately biasing both signal estimation and noise measurements. These effects are not independent. The SFR degradation and NPS inflation caused by localization error compound their impact on information capacity.

The LPF method improves robustness by reducing high-frequency noise prior to localization, thereby reducing both variance and bias in the estimated edge position. The matched filter incorporates an expected edge profile to produce a signal-informed estimate of edge position and achieves similarly low aggregate localization error at the precision reported here. Both methods substantially outperform centroid in the downstream metrics as well, reducing both SFR-area and NPS-area errors and their spread. Overall, both LPF and matched filter method produce SFR and NPS measurements that more closely reflect ground-truth system behavior than the centroid method.

These findings have important implications for information-based image quality metrics. Because information capacity is derived from both SFR and NPS, it is particularly sensitive to errors in edge localization. The results show that a centroid-based localization approach can lead to systematic underestimation of information capacity due to simultaneous reduction in high-frequency signal and overestimation of low-frequency noise. Given the demonstrated correlation between information capacity and machine vision performance, such errors may lead to incorrect predictions of system-level performance in practical applications.

From a standards perspective, this work highlights a limitation in the current ISO 12233 e-SFR framework. As information metrics become more prominent through standards such as ISO/WD 23654, the accuracy of edge localization becomes increasingly critical. The results suggest that improvements in localization methodology may be necessary to ensure consistency and reliability in both resolution and information measurements. For practical implementations, these results suggest that replacing centroid localization with either LPF or matched filtering can substantially reduce both bias and variability in SFR and information-based metrics without requiring changes to the remainder of the ISO 12233 e-SFR algorithm.

Several practical considerations should be addressed. The matched filter approach requires a correlation calculation between the template ESF and each row of the slanted edge ROI. This is much more computationally costly than the LPF and centroid approaches to edge localization. This study does not indicate a clear advantage of the matched filter approach over the LPF method given their similar aggregate performance. Furthermore, this study is based on simulated data and does not include validation on real imaging systems. Effects such as sharpening, compression, and nonlinear ISP processing were not modeled and may influence localization behavior in practical systems. The results therefore isolate the impact of localization error but may not capture all interactions present in real-world imaging pipelines.

Overall, this work demonstrates that edge localization is not merely an implementation detail, but a fundamental component of the measurement process that directly impacts both traditional and modern image quality metrics. Addressing localization error is therefore essential for improving the reliability of SFR measurements and for ensuring that information-based metrics accurately reflect system performance.

Conclusion

This work demonstrates that edge localization is a significant and previously under-characterized source of error in ISO 12233 e-SFR analysis. Using controlled simulations with ground truth, we show that centroid-based localization introduces noise-dependent angular bias that propagates through SFR and NPS, resulting in systematic underestimation of information capacity. In contrast, LPF and matched filter approaches provide substantially improved robustness relative to centroid localization, with both methods producing aggregate results much closer to ground truth across the conditions evaluated.

These findings have important implications for both standards-based measurement and machine vision evaluation. As information metrics such as those proposed in ISO/WD 23654 become more widely adopted, accurate edge localization becomes critical for reliable system characterization. Incorporating improved localization methods into standards frameworks may significantly enhance the accuracy and consistency of image quality metrics.

References

[1] "ISO 12233:2024 Digital cameras — Resolution and spatial frequency responses," ISO 12233:2024, 2024, [Online]. Available: https://www.iso.org/standard/88626.html

[2] J. B. Phillips and H. Eliasson, "Objective Image Quality Assessment - Theory and Practice," in *Camera Image Quality Benchmarking*, 1st ed., Hoboken, NJ: John Wiley and Sons, pp. 167–225, 2018, DOI: 10.1002/9781119054504.ch6.

[3] K. Nishi, "Does the slanted-edge method provide the true value of spatial frequency response?," *J. Opt. Soc. Am. A*, vol. 40, no. 2, pp. 259, 2023, DOI: 10.1364/JOSAA.478864.

[4] J. K. M. Roland, "A study of slanted-edge MTF stability and repeatability," presented at the IS&T/SPIE Electronic Imaging, (San Francisco, California, USA, 2015), pp. 93960L, DOI: 10.1117/12.2077755.

[5] ISO/TC 42, "Digital imaging — Image information metrics," ISO/WD 23654, Working Draft 1, 2026. https://www.iso.org/standard/87530.html

[6] N. L. Koren, "Image Information Metrics from Slanted Edges: A Toolkit of Metrics to Aid Object Recognition, Machine Vision, and Artificial Intelligence Systems,", 2024, DOI: 10.2352/EI.2024.36.9.IQSP-256.

[7] D. Geever *et al.*, "Information Capacity as a Predictor of Perception Performance," *IEEE Open J. Veh. Technol.*, vol. 7, pp. 708–722, 2026, DOI: 10.1109/OJVT.2026.3655075.

[8] P. D. Burns and D. Williams, "Camera Resolution and Distortion: Advanced Edge Fitting," *ei*, vol. 30, no. 12, pp. 171-1-171–5, 2018, DOI: 10.2352/ISSN.2470-1173.2018.12.IQSP-171.

[9] P. D. Burns, D. Williams, J. Griffith, H. Hall, and S. Cahall, "Application of ISO Standard Methods to Optical Design for Image Capture," *ei*, vol. 32, no. 9, pp. 240-1-240–7, 2020, DOI: 10.2352/ISSN.2470-1173.2020.9.IQSP-240.

[10] N. R. Rypkema, "A Straightforward Derivation of the Matched Filter," Open Science Framework, 2019, DOI: 10.31219/osf.io/gsjx3.

[11] H. H. Barrett and K. J. Myers, *Foundations of Image Science*: Wiley-Interscience, 2004.

[12] J. T. Bushberg, J. A. Seibert, E. M. Jr. Leidholdt, and J. M. Boone, "Image Quality," in *The Essential Physics of Medical Imaging*, 4th ed., Philadelphia, PA: Lippincott Williams & Wilkins, pp. 72–108, 2020.

Author Biography

Sarah Kerr is an Imaging Scientist at Imatest LLC, where she develops and validates image quality metrics and measurement methodologies for digital camera systems. She serves as Co-Project Leader for ISO 23654 (Digital Imaging - Information Metrics) within ISO/TC 42 and contributes to international standards development in digital imaging performance. She holds B.S. and M.S. degrees in physics and works at the intersection of imaging standards, quantitative analysis, and software implementation.

JOIN US AT THE NEXT EI!

electronic IMAGING

Imaging across applications . . . Where industry and academia meet!

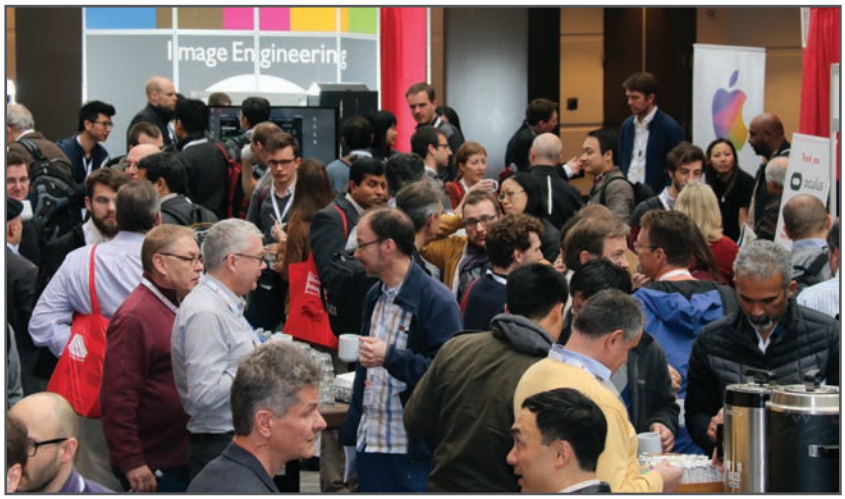

• SHORT COURSES • EXHIBITS • DEMONSTRATION SESSION • PLENARY TALKS •
• INTERACTIVE PAPER SESSION • SPECIAL EVENTS • TECHNICAL SESSIONS •

www.electronicimaging.org

ADVANCING IMAGING SCIENCE 75 1947 IS&T 2022 imaging.org